

## Original Research Article

# Prediction of the Therapeutic Response to Neoadjuvant Chemotherapy for Rectal Cancer Using a Deep Learning Model

Shunsuke Kubota<sup>1)</sup>, Taiichi Wakiya<sup>1)</sup>, Hajime Morohashi<sup>1)</sup>, Takuya Miura<sup>1)</sup>, Taishu Kanda<sup>1)</sup>, Masashi Matsuzaka<sup>2)</sup>, Yoshihiro Sasaki<sup>2)</sup>, Yoshiyuki Sakamoto<sup>1)</sup> and Kenichi Hakamada<sup>1)</sup>

1) Department of Gastroenterological Surgery, Hirosaki University Graduate School of Medicine, Hirosaki, Japan

2) Department of Medical Informatics, Hirosaki University Hospital, Hirosaki, Japan

### Abstract

**Objectives:** Predicting the response to chemotherapy can lead to the optimization of neoadjuvant chemotherapy (NAC). The present study aimed to develop a non-invasive prediction model of therapeutic response to NAC for rectal cancer (RC).

**Methods:** A dataset of the prechemotherapy computed tomography (CT) images of 57 patients from multiple institutions who underwent rectal surgery after three courses of S-1 and oxaliplatin (SOX) NAC for RC was collected. The therapeutic response to NAC was pathologically confirmed. It was then predicted whether they were pathologic responders or non-responders. Cases were divided into training, validation and test datasets. A CT patch-based predictive model was developed using a residual convolutional neural network and the predictive performance was evaluated. Binary logistic regression analysis of prechemotherapy clinical factors showed that none of the independent variables were significantly associated with the non-responders.

**Results:** Among the 49 patients in the training and validation datasets, there were 21 (42.9%) and 28 (57.1%) responders and non-responders, respectively. A total of 3,857 patches were extracted from the 49 patients. In the validation dataset, the average sensitivity, specificity and accuracy was 97.3, 95.7 and 96.8%, respectively. Furthermore, the area under the receiver operating characteristic curve (AUC) was 0.994 (95% CI, 0.991-0.997;  $P < 0.001$ ). In the test dataset, which included 750 patches from 8 patients, the predictive model demonstrated high specificity (89.9%) and the AUC was 0.846 (95% CI, 0.817-0.875;  $P < 0.001$ ).

**Conclusions:** The non-invasive deep learning model using prechemotherapy CT images exhibited high predictive performance in predicting the pathological therapeutic response to SOX NAC.

### Keywords

computational prediction, CT, machine learning, deep learning, NAC, RC

J Anus Rectum Colon 2025; 9(2): 202-212

## Introduction

For rectal cancer (RC) patients, both local and distant recurrence after curative surgery are major factors worsening long-term prognosis. To control recurrence, a negative cir-

cumferential resection margin is required. Neoadjuvant therapy (NAT) followed by total mesorectal excision (TME) comprises the standard of care for RC found in multiple guidelines[1-4]. To achieve better outcomes for RC patients, various regimens have been devised for NAT[5-9]. Although

neoadjuvant chemoradiotherapy (NACRT) is recommended in several guidelines, radiation has negative effects including bowel, urinary and sexual dysfunctions. Neoadjuvant chemotherapy (NAC) is one NAT regimen that prevents the heretofore inevitable radiation toxicity. In terms of pathological tumor response, R0 resection rate, local relapse, and distant metastasis, NAC has been demonstrated to be non-inferior to NACRT[8]. Other randomized control trials revealed that NAC without radiation had equal oncologic outcomes and provided better anorectal function, which demonstrated NAC could be a treatment option for patients who do not wish to undergo radiation[10,11].

Our recent prospective multicenter phase 2 study has also demonstrated the feasibility and efficacy of S-1 and oxaliplatin (SOX) NAC with TME for resectable lower RC[12]. SOX NAC resulting in a high rate of pathological complete response (CR, 19.2%). However, approximately half of the cases showed no effective response in our previous study[12]. Tumor response to NAT is associated with good long-term outcomes in patients with RC[11-14]. Thus, further research and solutions are required for patients with an unfavorable response to SOX NAC.

Theoretically, the prediction of a patient's response to this protocol can lead to the optimization of NAC. The optimization of NAC would yield several valuable benefits, including minimizing the adverse events and cost of ineffective therapy, avoiding treatment delays with poor-responders, and providing the option of switching to other chemotherapy drugs. Therefore, there is a need to establish a prediction model for therapeutic response to chemotherapy.

So far, many studies have been conducted to predict patient response to NAT in RC[15-21]. Nonetheless, no reliable clinical application has been established. To achieve a more precise prediction model, much attention is being placed on a machine learning approach. The effectiveness of machine learning in predicting responses to NACRT for RC has been reported previously[22-24]. These researchers have succeeded in predicting the pathological CR after NACRT. However, because these reports have focused on predicting the response to NAT with radiation, their models were inherently not intended to predict the response to simple chemotherapy drugs. In other words, no prediction model that contributes to the optimization of chemotherapy is presently available. Thus, this study aimed to develop a prediction model for therapeutic response to NAC for RC. We have applied deep learning (DL), a subset of machine learning, and successfully developed a prediction model for therapeutic response to SOX NAC using prechemotherapy computed tomography (CT) images.

## Methods

### *Patients and study design*

This retrospective, observational study was approved by the Committee of Medical Ethics of Hirosaki University Graduate School of Medicine (reference no. 2021-051). Informed consent was obtained in the form of an opt-out system on our website (<https://www.med.hirosaki-u.ac.jp/hospital/outline/resarch/resarch.html>), with the approval of the Committee. Our study did not include minors. This study was designed and carried out in accordance with the Declaration of Helsinki. The study utilized data from participants in a prior multi-center collaborative research project, which had been ethically approved by the Committee (reference no. 2018-A-012; Aomori, Japan). All collected data were managed with the highest regard for participant privacy and confidentiality.

Inclusion criteria for this study specified the following: 1) there should be a histologically confirmed adenocarcinoma; 2) the distal border of the tumor must be located at or below the peritoneal reflection, along with tumors located 5 cm from the anal verge (low rectal cancer) and tumors that are between 5 and 10 cm located 5 cm from the anal verge (middle rectal cancer); 3) the tumor must be categorized as cT3-4N0-2M0, which can be resected; 4) the patient must be between 20 and 80 years old; 5) the Eastern Cooperative Oncology Group Performance Status Scale should be 0 or 1; 6) organ function, including a leukocyte count of 3000 to 12,000 mm<sup>3</sup>, a neutrophil count of  $\geq 1500$  mm<sup>3</sup>, a platelet count of  $\geq 100,000$  mm<sup>3</sup>, a hemoglobin concentration of  $\geq 9.0$  g/dL, aspartate aminotransferase and alanine aminotransferase levels of  $\leq 100$  IU/L, a serum total bilirubin level of  $\leq 2.0$  mg/dL, and a serum creatinine level of  $\leq 1.2$  mg/dL, must be preserved; and 7) written informed consent must be provided by the patient. These criteria were validated in our previous study[10].

A total of 58 patients who underwent rectal surgery, with curative intent, for RC at multiple institutions between April 2015 and September 2019 were considered. We excluded one patient who could not complete the NAC regimen because of an adverse effect leading to thrombocytopenia. Fifty-seven patients who completed NAC followed by surgery were included in this study. The recruitment process of study participants is shown in Figure 1. All patients had pathologically confirmed therapeutic response to NAC by board-certified pathologists. The baseline clinicopathologic data used in this study were collected prospectively through another clinical study. In total, 49 patients comprised the training and validation sets and 8 comprised the test set. Our workflow is shown in Figure 2. The division was performed to achieve a generally acceptable ratio for training and test sets. The test dataset specifically included cases from Hospi-

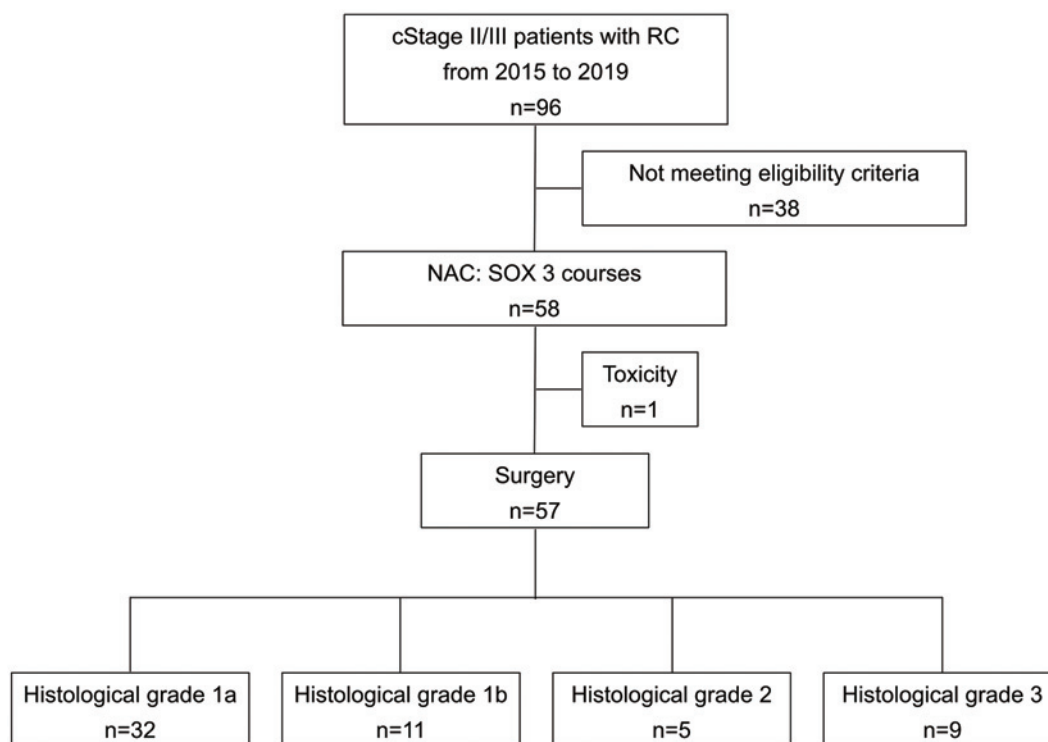


**Figure 1** Process of recruitment of study participants. NAC, neoadjuvant chemotherapy; RC, rectal cancer; SOX, S-1 and oxaliplatin

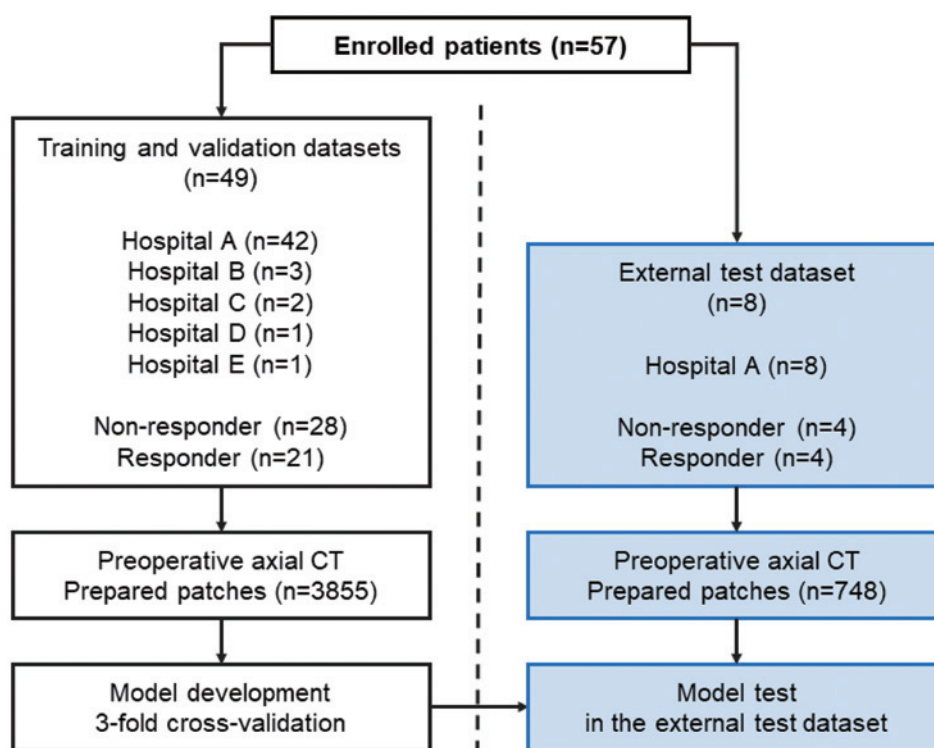


**Figure 2.** Study workflow and methodological process. Hospital A, Hirosaki University Hospital, Hirosaki, Japan; Hospital B, Narumi Hospital, Hirosaki, Japan; Hospital C, Tsugaru General Hospital, Goshogawara, Japan; Hospital D, Hirosaki Municipal Hospital, Hirosaki, Japan; Hospital E, Kuroishi General Hospital, Kuroishi, Japan. CT, computed tomography

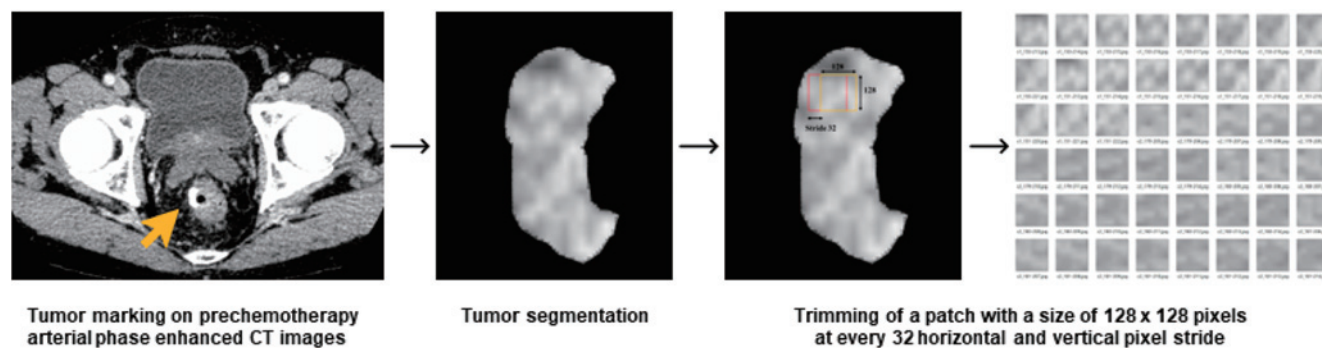


**Figure 3.** Process of preparing a dataset. Yellow arrow, tumor. CT, computed tomography. A patch measuring 128×128 pixels with a 32-pixel stride was extracted from the entire segmented tumor area. A stride was performed horizontally and vertically for data augmentation. For example, c\_1-150-214.jpg (top row, second from the left) was cut out by shifting 32 pixels downward from c\_1-150-213.jpg (top row, far left).

tal A, which had the highest recruitment rate. Furthermore, the test dataset maintained a balanced ratio of responders to non-responders at 1:1. The division was randomized to meet these criteria while ensuring a representative sample distribution.

### Neoadjuvant chemotherapy

Three courses of S-1, an oral anticancer agent containing 2 biochemical modulators for 5-fluorouracil (5-FU) and tegafur, a metabolically activated prodrug of 5-FU, and oxaliplatin (SOX) NAC were administered before surgery. S-1 was administered orally at 80 mg/m<sup>2</sup>/day for 14 consecutive days, followed by a 7-day resting period. Oxaliplatin was given intravenously on the first day at a dose of 130 mg/m<sup>2</sup>/day. The duration of one cycle was considered to be 21 days, and, as stated, there were three cycles.

### Surgery

Surgery was carried out three to eight weeks after chemotherapy ended. The types of operations performed included low anterior resection, intersphincteric resection, Hartmann's operation, and abdominoperineal resection, which included total TME. All patients underwent laparoscopic or robotic-assisted laparoscopic surgery.

### Grading of the histological response to NAC

Pathologic tumor response to NAC, based on the Japanese Society for Cancer of the Colon and Rectum standards[25], was classified as follows: Grade 0, no tumor cell necrosis or degeneration in response to treatment is observed; Grade 1a, tumor cell necrosis or degeneration is present in less than one-third of the entire lesion; Grade 1b, tumor cell necrosis, degeneration, and/or a lytic change is present in more than one-third but less than two-thirds of the entire lesion; Grade 2, prominent tumor cell necrosis, degeneration, a lytic change, and/or a disappearance is present in more than two-thirds of the entire lesion, but viable tumor cells remain;

Grade 3, necrosis and/or a lytic change is present throughout the entire lesion and has been replaced by fibrosis with or without a granulomatous change; no viable tumor cells are observed. Pathological assessment was performed by board-certified pathologists.

### Prediction label definitions

In this study, we predicted the pathological responder vs. the non-responder. The non-responder was defined as someone with a histological response of grade 0 to 1a. The responder was defined as having a histological response of grade 1b to 3.

### CT acquisition and tumor segmentation

The dataset preparation process is shown in Figure 3. The prechemotherapy axial arterial phase enhanced CT images for each case used for each case of this study were obtained from the multicenter database where they have been stored. The spatial resolution of the CT images has been adjusted to 0.0126 mm/pixel. Radiological assessment was performed by board-certified radiologists blinded to the diagnoses of the patients. Two surgeons and two medical students performed CT acquisition and tumor segmentation based on the radiological assessment. This tumor segmentation method was validated in our previous studies[25-27]. Using a commercial viewer (ShadeQuest/ViewR, Fujifilm, Japan), CT image showing the tumor area was selected and exported into a TIFF file of 999 dots per inch. The TIFF images were further processed with Adobe Illustrator. The entire tumor region was manually marked for segmentation and saved at 2000 pixels per inch (ppi). We also re-saved the main image at 2000 ppi.

### Preparation of dataset

We trimmed a patch with a size of 128 × 128 pixels with a 32-pixel stride from the entire segmented tumor area. When the intersection between a patch and the segmentation



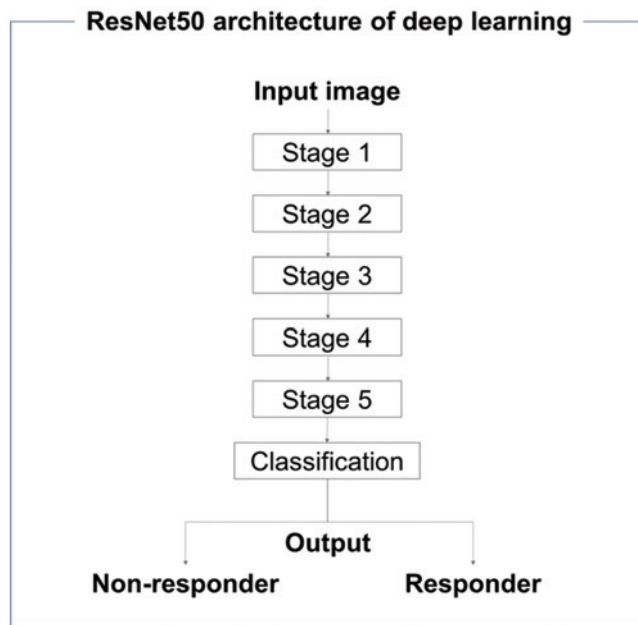


**Figure 4.** Architecture of the convolutional neural network. Stage 1 consisted of an initial convolution layer, batch normalization, a rectified linear unit and max pooling. Stages 2-5 comprised residual blocks that included convolutional layers and identity layers. ResNet, residual convolutional neural network

mask had less than a  $128 \times 128 \times 0.999$  pixel count, the patch was automatically excluded from analysis. Finally, 4,607 patches were obtained from 57 patients in the current study.

#### Architecture of the convolutional neural network

Deep learning was performed using CT images from both the responder and non-responder groups. A convolutional neural network was used to obtain relevant feature representations of the images of the responder and non-responder groups. ResNet50[26] and Pytorch (a python library) were utilized (available at: <https://github.com/pytorch/pytorch>). ResNet50 features a sophisticated convolutional neural network architecture, complete with shortcut connections that facilitate seamless residual learning. Its components include (1) input layers, (2) convolutional layers for identifying key features, (3) residual blocks for enhancing network depth, (4) pooling layers for subsampling, (5) fully connected layers for recognizing patterns relevant to classification or regression tasks, and culminates in an output layer for final predictions. We did not use a pretrained model. The original acquired images of  $128 \times 128$  pixels were converted into images of  $224 \times 224$  pixels. We tuned the hyperparameters as follows: number of training epochs, 50; batch size, 128; learning rate, 0.00025 via trial and error; and number of outer layers, two classes. The patches trimmed from the CT images were inputted into the convolutional neural network architecture and they were classified into responder or non-

responder (Figure 4).

#### Evaluation methods

In designing the evaluation methods for this study, we followed the practices established in our previous studies[27-29]. We employed a cross-validation approach to ensure robustness and minimize bias in our machine learning evaluations[30]. Cross-validation involves randomly splitting the training and validation datasets into multiple folds, with one fold used for validation while the others are utilized for training. In this study, this process was repeated three times, with different folds each time, to obtain a more comprehensive assessment. The key objective was to maintain an equal proportion of patients with responder or non-responder status in each fold, ensuring a balanced representation. Next, we evaluated predictive performance using the test datasets. The final results were obtained by averaging the outcomes across the folds, and the standard deviation (SD) was calculated. To measure the effectiveness of our model, we employed various metrics, including accuracy, sensitivity, specificity, positive predictive values, and negative predictive values. The evaluation was further substantiated by receiver operating characteristic (ROC) curves, and the values for the area under the curve (AUC) were computed.

#### Statistical analysis

Continuous variables were expressed as the medians (ranges) and analyzed using nonparametric methods for non-normally distributed data (Mann-Whitney U-test). Categorical variables were reported as numbers (percentages) and analyzed using the chi-squared test or Fisher's exact test, as appropriate. Mann-Whitney U,  $\chi^2$  and Fisher's exact tests were used to identify variables significantly linked to the non-responder status. Those with significant associations ( $P < 0.050$ ) were then included in a binary logistic regression analysis. The statistical analyses were performed using IBM SPSS Statistics for Windows, Version 26.0 (IBM Corp, Armonk, NY, USA).

## Results

#### Comparison of the prechemotherapy characteristics between the groups

The prechemotherapy characteristics of the 57 enrolled RC patients are shown in Table 1. Of the 57 patients, 25 (43.9%) were included in the responder group, with 32 (56.1%) in the non-responder group. In the responder group, on average, the age was higher, and the body weight was lower than the non-responder group. There were no significant differences in tumor biomarkers such as carbohydrate antigen 19-9 or carcinoembryonic antigen between the groups. The non-responder group showed a greater preva-

**Table 1.** Comparison of the Prechemotherapy Characteristics.

Characteristics	All cases (n=57)	Responder (n=25)	Non-responder (n=32)	P-value	Logistic regression analysis		
					Odds ratio	95% CI	P- value
Sex, n (%)				0.508 <sup>a</sup>			
Male	46 (80.7)	19 (76.0)	27 (84.3)				
Female	11 (19.3)	6 (24.0)	5 (15.6)				
Age, years	65 (34-77)	69 (37-77)	61 (34-77)	0.015	0.978	0.917-1.043	0.495
Body height, cm	165 (144-185)	162 (144-176)	167 (146-185)	0.002	1.056	0.956-1.166	0.284
Body weight, kg	60 (40-87)	56 (40-74)	64 (49-87)	0.023	1.074	0.985-1.172	0.106
Body mass index, kg/m <sup>2</sup>	21.2 (16.9-30.4)	21.2 (16.9-30.4)	21.3 (17.9-29.2)	0.760			
Laboratory values							
CA19-9, U/ml	10 (1-420)	11 (1-420)	9 (1-90)	0.562			
CEA, ng/ml	4.1 (0.7-253.8)	4.1 (1.2-253.8)	4.2 (0.7-95.8)	0.994			
CA19-9/CEA	2.50 (0.02-17.22)	3.23 (0.02-9.09)	2.10 (0.12-17.22)	0.520			
Tumor location, n (%)				>0.999 <sup>a</sup>			
Ra	2 (3.5)	1 (4.0)	1 (3.1)				
Rb	55 (96.5)	24 (96.0)	31 (96.9)				
Initial T stage, n (%)				0.735 <sup>a</sup>			
cT3	47 (82.5)	20 (80.0)	27 (84.3)				
cT4	10 (17.5)	5 (20.0)	5 (15.6)				
Initial N stage, n (%)				0.008	2.589	0.127-52.971	0.537
cN0	23 (40.4)	15 (60.0)	8 (25.0)				
cN1-3	34 (59.6)	10 (40.0)	24 (75.0)				
Initial clinical stage, n (%)				0.008	2.267	0.093-55.181	0.615
II	21 (36.8)	14 (56.0)	7 (21.9)				
III	36 (63.2)	11 (44.0)	25 (78.1)				
Tumor histology, n (%)				0.499 <sup>a</sup>			
Well/moderately differentiated	55 (96.5)	25 (100)	30 (93.8)				
Poorly differentiated	0 (0.0)	0 (0.0)	0 (0.0)				
Mucinous	2 (3.5)	0 (0.0)	2 (6.2)				
Stoma construction before NAC, n (%)				0.686 <sup>a</sup>			
Yes	6 (10.5)	2 (8.0)	4 (12.5)				
No	51 (89.5)	23 (92.0)	28 (87.5)				

<sup>a</sup>Fisher's exact test was performed, while other comparisons for categorical variables were carried out using the  $\chi^2$  test. Continuous variables are presented as the median (range) and were analyzed using the Mann-Whitney U-test. Categorical variables are reported as the number (percentage) and were analyzed using the  $\chi^2$  test or Fisher's exact test, as appropriate. Mann-Whitney U,  $\chi^2$  and Fisher's exact tests were used to identify variables significantly associated with non-responder status. Those with significant associations ( $P < 0.05$ ) were then included in a binary logistic regression analysis. CA19-9, carbohydrate antigen 19-9; CEA, carcinoembryonic antigen; NAC, neoadjuvant chemotherapy; Ra, upper rectum; Rb, lower rectum

lence of clinical lymph node metastasis (40.0 vs. 75.0%,  $P = 0.008$ ). Consequently, highly advanced cases were more common in the non-responder group.

### Binary logistic regression analysis

To predict non-responders, we performed a binary logistic regression analysis. Significant variables linked with the non-responder, which were found through a univariate analysis ( $P < 0.050$ ), as listed in Table 1, were entered into a binary regression analysis. Multivariate analysis showed that none of the independent variables were significantly as-

sociated with the dependent variable (all  $P > 0.050$ ). These results indicated that there was a difficulty in predicting the response to NAC from independent variables in this cohort.

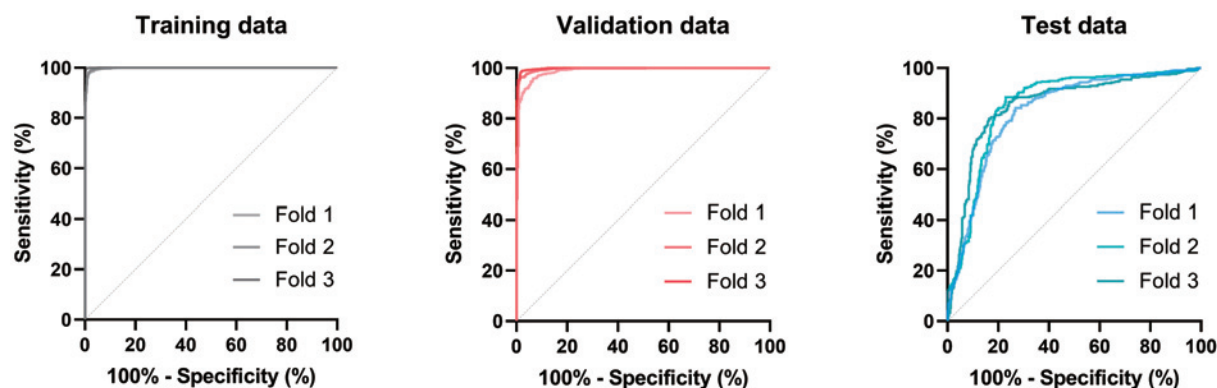
### Performance of the DL model in the training and validation datasets

Next, we developed a model to predict the response to chemotherapy from prechemotherapy CT images. Of the 49 patients that comprised the training and validation datasets, a total of 1,179 patches were obtained from the 21 responders. Then, a total of 2,678 patches were obtained from the

**Table 2.** Performance of the Deep Learning Model for Prediction of Non-Responders in the Training and Validation Datasets.

Metric	Fold 1, %	Fold 2, %	Fold 3, %	Mean, %	SD, %
Training dataset					
Sensitivity	98.4	98.7	99.6	98.9	0.6
Specificity	97.4	98.1	99.4	98.3	1.0
False negative rate	1.6	1.3	0.4	1.1	0.6
False positive rate	2.6	1.9	0.6	1.7	1.0
Positive predictive value	98.9	99.2	99.7	99.3	0.4
Negative predictive value	96.3	97.1	99.1	97.5	1.4
Accuracy	98.1	98.5	99.5	98.7	0.7
Validation dataset					
Sensitivity	95.8	97.0	99.1	97.3	1.7
Specificity	93.7	96.6	97.0	95.7	1.8
False negative rate	4.2	3.0	0.9	2.7	1.7
False positive rate	6.3	3.4	3.0	4.3	1.8
Positive predictive value	97.3	98.5	98.7	98.2	0.7
Negative predictive value	90.3	93.1	98.0	93.8	3.9
Accuracy	95.2	96.9	98.4	96.8	1.6

Fold refers to a subset of data used in cross-validation.

**Figure 5.** ROC curves of the deep learning model. ROC curves showing the performance of each dataset. Each fold is a subset of data used in cross-validation. ROC, receiver operating characteristic

28 non-responders. Finally, a total of 3,857 patches were extracted from the 49 patients in the training and validation datasets, representing cases from all five participating institutions. The model achieved an AUC of 0.999 (95% CI: 0.998-0.999,  $P < 0.001$ ) in the training dataset. The average accuracy of the predicting model for the non-responder was 96.8% for the validation dataset. The average sensitivity, specificity, and positive and negative predictive values were 97.3%, 95.7%, 98.2%, and 93.8%, respectively (Table 2). The model achieved an AUC of 0.994 (95% CI: 0.991-0.997,  $P < 0.001$ ) in the validation dataset (Figure 5).

#### Performance of the DL model in the test datasets

We then evaluated the performance of the developing model using the test dataset. The test dataset included 396 patches from four responders and 354 patches from four

non-responders. Likewise, the model showed acceptable predicting performance in the test dataset. Although further improvement of the sensitivity was required, the developing model showed both high specificity (89.9%) and high positive predictive value (93.3%) (Table 3). The DL model achieved an acceptable AUC of 0.846 (95% CI: 0.817-0.875,  $P < 0.001$ ) even in the test dataset (Figure 5). These results suggested that the developing model was suitable for identifying patients with an unfavorable response to SOX NAC.

#### Discussion

We applied this noninvasive deep learning model to predict pathological therapeutic response to SOX NAC for RC. We have successfully demonstrated high performance in prediction using prechemotherapy CT images. Our models can

**Table 3.** Performance of the Deep Learning Model for Prediction of Non-Responders in the Test Dataset.

Metric	Fold 1, %	Fold 2, %	Fold 3, %	Mean, %	SD, %
Sensitivity	64.4	66.5	62.0	64.3	2.3
Specificity	88.8	92.7	88.2	89.9	2.4
False negative rate	35.6	33.5	38.0	35.7	2.3
False positive rate	11.2	7.3	11.8	10.1	2.4
Positive predictive value	92.4	94.9	92.7	93.3	1.4
Negative predictive value	54.3	57.3	49.2	53.6	4.1
Accuracy	72.3	75.1	69.7	72.4	2.7

Fold refers to a subset of data used in cross-validation.

contribute to the optimization of SOX NAC for RC. Furthermore, this study can offer a novel insight into personalized treatment strategies, including the optimization of chemotherapy, in RC management.

Machine learning has gained significant attention in predicting treatment outcomes in multiple cancer fields. In RC, machine learning has been reported efficient in predicting a pathological CR after NACRT with high accuracy[22-24]. These studies showed the advantage of this approach in identifying pathological CR patients who have a good prognosis and may benefit from conservative therapy such as a watch-and-wait approach. However, those models were not designed to predict response to chemotherapy drugs. In contrast, we intended to predict the therapeutic response to chemotherapy drugs. Part of the reason that we wanted to do this is that the current chemotherapy regimen has been established based on the results of past major clinical studies, rather than on individual patient information. Unfortunately, the conventional selection process of chemotherapy regimens has been far from focused on chemotherapy optimization or personalized medicine. Thus, we constructed a prediction model to optimize drug regimens with personalization in mind.

Our noninvasive prediction model demonstrated high performance with all therapeutic responses. The implication of this is that it can be applied to the clinical situation from two perspectives. The prediction of the patient being a responder can push us to select SOX regimen for NAC. Furthermore, the prediction of a non-responder may have equal or greater significance in real-world clinical settings. Generally, if there is ultimately no response, NAT can potentially cause the patient to miss the opportunity for surgery due to tumor growth. Especially in rectal surgery, tumor growth while undergoing NAT may make it harder to perform surgery and get a sufficient circumferential margin (CRM). Radical resection with a sufficient CRM is needed to prevent postoperative local recurrence[31,32]. Additionally, tumor growth during NAT may increase the combined organ resection rate and decrease the sphincter preservation rate. In clinical situations, other regimens should be selected for the

patients who are predicted to be poor responders to SOX NAC. Having access to this predictive information can help avoid the undesired consequences of tumor growth due to inadequate regimens as described above. In other words, our prediction model can contribute to the optimization of SOX NAC for RC patients.

Deep learning models, such as convolutional neural networks, applied in this study, examine various visual patterns or features in CT images. These features generally include edges and lines, color variations, texture, shapes and patterns, and hierarchical features. However, the specific nature of these extracted features remains unclear. This limitation is intrinsic to deep learning models, which currently lack the interpretability needed to fully elucidate the significance of these features. These features may indicate higher malignant potential or could relate to a certain mechanism underlying chemotherapy resistance. Continued advancements in explainable deep learning approaches hold promise for uncovering the so-called “black box” of these models, enabling more transparent interpretation of complex features.

It is feasible to build a predictive model utilizing contrast-enhanced CT images as well as non-contrast CT images. In fact, we have successfully developed a model to predict postoperative recurrence of intrahepatic cholangiocarcinoma using preoperative non-contrast CT images[27]. However, unlike liver tumors, it is quite difficult to accurately segment colorectal cancer areas on non-contrast CT images. Therefore, in this study, we constructed a model using contrast-enhanced CT images. That is, the model constructed in this study can be applied only to patients who have contrast-enhanced CT images.

In this study, we used SOX regimens. SOX is a convenient oral drug regimen that helps maintain quality of life for patients because it does not need an infusion pump. We have demonstrated the effectiveness of SOX NAC in our previous study[12]. In other studies, SOX was shown to be comparable to CapeOX in advanced colorectal cancer[33]. As for a SOX + Bevacizumab regimen, non-inferiority to mFOLFOX6 + Bevacizumab was demonstrated in advanced colorectal cancer as well[34].



This study has several limitations. First, the patient population was not large. To accommodate the heterogeneity of RCs and the diversity of clinical practice and patient responses, a large cohort is ideal. On the other hand, our results demonstrated the prospects of the methodology using CT images and deep learning. Thus, if we had access to a huge database, such as national or regional datasets, we could achieve even higher prediction accuracy. Furthermore, this study included only RC patients receiving SOX NAC. This indicates a limited breadth of representation of chemotherapy regimens. Many chemotherapy regimens have been shown to be effective for RC. In other words, a predictive model for all of the regimens is needed to realize true optimization of chemotherapy regimens for RC. To achieve this goal, it is desirable to establish an aggregation center for predictive models that are generated at institutions around the world using various chemotherapeutic strategies. We hope that this pilot study will be the beginning of that process. Moreover, the influence of molecular biological features, including BRAF and RAS, was not considered in this study. It is difficult to discuss them because molecular biological exams were not mandatory during the period in which this study was conducted. In addition, how the time after NAC affected the pathological responses was unclear in this study. With regard to all cases in this study, operations were performed within 4-8 weeks after completion of NAC. Although we cannot ignore the variation, its effect was considered minimal because the waiting period for each case did not differ significantly. Finally, there was the question of possible lack of homogeneity in CT techniques. In fact, however, our model attained high predictive performance. These results suggested that the relative heterogeneity of CT techniques may not be a big concern because of the successful handling, through deep learning, of the enormous information available from CT images. Certainly, homogeneity of CT techniques would be preferable. Nevertheless, nowhere, in a real clinical setting, would it be practical for all patients to undergo CT exams using the same scanner and technique. Hence, considered from a different perspective, the use of CT images is one of the strengths of our study. Generally, CT exams are more widely used than MRI exams and are less expensive. With the intention of supporting patients in resource-limited regions where MRI is challenging, as well as those who cannot undergo MRI due to implanted medical devices, we opted for CT. NAC is also more widely available than NACRT. Nowadays, RC is one of the more deadly cancers worldwide[35]. Our concept of combining CT images and NAC in RC management enhances the general relevance and feasibility in clinical applications worldwide.

In conclusion, our deep learning model, using prechemotherapy CT images of RC, exhibited high predictive performance in projecting therapeutic response to SOX NAC. The present study has provided a novel approach to predict

treatment response to NAC for RC. This approach can contribute to personalized strategies in RC management. The hope for the future is to conduct a study with a large dataset to establish a clinical application.

#### Acknowledgements

We sincerely thank Professor Shari Joy Berman (Hirosaki University Graduate School of Medicine, Hirosaki, Aomori, Japan) for professionally editing the English draft of this manuscript. We are sincerely grateful to Sotaro Ichiyama and Kenji Soma at the Hirosaki University School of Medicine for collecting the clinical data.

#### Conflicts of Interest

There are no conflicts of interest.

#### Author Contributions

SK and TW contributed to the conception and design of the study. SK, HM, TM, TK and YSak performed surgical resection. SK, TW, HM, TM, TK, MM, YSas, YSak and KH collected the clinical data. SK, TW, HM, TM, TK, MM, YSas, YSak and KH analyzed and interpreted the data. SK and TW wrote the first draft of the manuscript. HM, TM, TK, MM, YSas, YSak and KH contributed to the review and/or critical revision of the manuscript. All authors agreed to be accountable for all aspects of the work in ensuring that questions related to the accuracy or integrity of any part of the work are appropriately investigated and resolved. SK and HM confirm the authenticity of all the raw data. All authors have read and approved the final version of the manuscript. Shunsuke Kubota and Taiichi Wakiya contributed equally to this work.

#### Approval by Institutional Review Board (IRB)

The present study was approved by the Committee of Medical Ethics of Hirosaki University Graduate School of Medicine (reference no. 2021-051; Aomori, Japan). The present study did not include minors. The present study was designed and carried out in accordance with the Declaration of Helsinki.

#### Availability of Data and Materials

The data generated in the present study may be requested from the corresponding author.

#### Patient Consent for Publication

Informed consent for publication was obtained in the form of an opt-out function on our website, with the approval of the Committee of Medical Ethics of Hirosaki University Graduate School of Medicine (Aomori, Japan).

#### Informed Consent

Informed consent was obtained in the form of an opt-out

function on our website, with the approval of the Committee of Medical Ethics of Hirosaki University Graduate School of Medicine.

## References

- Glynne-Jones R, Wyrwicz L, Tiret E, et al. Rectal cancer: ESMO Clinical Practice Guidelines for diagnosis, treatment and follow-up. *Annals of Oncology*. 2017 Jul; 28(suppl 4): iv22-40.
- Benson AB, Venook AP, Al-Hawary MM, et al. Rectal Cancer, Version 2. 2018, NCCN Clinical Practice Guidelines in Oncology. *Journal of the National Comprehensive Cancer Network*. 2018 Apr; 16(7): 874-901.
- You YN, Hardiman KM, Bafford A, et al. The American Society of Colon and Rectal Surgeons Clinical Practice Guidelines for the Management of Rectal Cancer. *Diseases of the Colon & Rectum*. 2020 Sep; 63(9): 1191-222.
- Hashiguchi Y, Muro K, Saito Y, et al. Japanese Society for Cancer of the Colon and Rectum (JSCCR) guidelines 2019 for the treatment of colorectal cancer. *Int J Clin Oncol*. 2020 Jan; 25(1): 1-42.
- Kasi A, Abbasi S, Handa S, et al. Total Neoadjuvant Therapy vs Standard Therapy in Locally Advanced Rectal Cancer: A Systematic Review and Meta-analysis. *JAMA Network Open*. 2020 Dec; 3(12): e2030097.
- Ali F, Keshinro A, Weiser MR. Advances in the treatment of locally advanced rectal cancer. *Ann Gastroenterol Surg*. 2020 Aug 30; 5(1): 32-8.
- Giunta EF, Bregni G, Pretta A, et al. Total neoadjuvant therapy for rectal cancer: Making sense of the results from the RAPIDO and PRODIGE 23 trials. *Cancer Treat Rev*. 2021 May; 96: 102177.
- Lin H, Wang L, Zhong X, et al. Meta-analysis of neoadjuvant chemotherapy versus neoadjuvant chemoradiotherapy for locally advanced rectal cancer. *World J Surg Oncol*. 2021 May; 19(1): 141.
- Toiyama Y, Kusunoki M. Changes in surgical therapies for rectal cancer over the past 100 years: A review. *Annals of Gastroenterological Surgery*. 2020 May; 4(4): 331-42.
- Deng Y, Chi P, Lan P, et al. Neoadjuvant Modified FOLFOX6 With or Without Radiation Versus Fluorouracil Plus Radiation for Locally Advanced Rectal Cancer: Final Results of the Chinese FOWARC Trial. *J Clin Oncol*. 2016 Feb; 31(6): 611-35.
- Schrag D, Shi Q, Weiser MR, et al. Preoperative Treatment of Locally Advanced Rectal Cancer. *N Engl J Med*. 2023 Jul; 389(4): 322-34.
- Sakamoto Y, Morohashi H, Miura T, et al. A Prospective Multicenter Phase II Study on the Feasibility and Efficacy of S-1 and Oxaliplatin Neoadjuvant Chemotherapy for Locally Advanced Rectal Cancer. *Dis Colon Rectum*. 2022 May; 65(5): 663-71.
- Fokas E, Liersch T, Fietkau R, et al. Tumor regression grading after preoperative chemoradiotherapy for locally advanced rectal carcinoma revisited: updated results of the CAO/ARO/AIO-94 trial. *J Clin Oncol*. 2014 May; 32(15): 1554-62.
- Maas M, Nelemans PJ, Valentini V, et al. Long-term outcome in patients with a pathological complete response after chemoradiation for rectal cancer: a pooled analysis of individual patient data. *Lancet Oncol*. 2010 Sep; 11(9): 835-44.
- Zorcolo L, Rosman AS, Restivo A, et al. Complete pathologic response after combined modality treatment for rectal cancer and long-term survival: a meta-analysis. *Ann Surg Oncol*. 2012 Sep; 19(9): 2822-32.
- Martin ST, Heneghan HM, Winter DC. Systematic review and meta-analysis of outcomes following pathological complete response to neoadjuvant chemoradiotherapy for rectal cancer. *Br J Surg*. 2012 Jul; 99(7): 918-28.
- Patel UB, Taylor F, Blomqvist L, et al. Magnetic Resonance Imaging-Detected Tumor Response for Locally Advanced Rectal Cancer Predicts Survival Outcomes: MERCURY Experience. *Journal of Clinical Oncology*. 2011 Oct; 29(28): 3753-60.
- Joye I, Deroose CM, Vandecaveye V, et al. The role of diffusion-weighted MRI and (18)F-FDG PET/CT in the prediction of pathologic complete response after radiochemotherapy for rectal cancer: A systematic review. *Radiotherapy and Oncology*. 2014 Nov; 113(2): 158-65.
- Li N, Dou L, Zhang Y, et al. Use of sequential endorectal US to predict the tumor response of preoperative chemoradiotherapy in rectal cancer. *Gastrointestinal Endoscopy*. 2017 Mar; 85(3): 669-74.
- Ryan JE, Warrier SK, Lynch AC, et al. Predicting pathological complete response to neoadjuvant chemoradiotherapy in locally advanced rectal cancer: a systematic review. *Colorectal Disease*. 2016 Mar; 18(3): 234-46.
- Daye D, Tanaka I, Jain R, et al. Predictive and Prognostic Molecular Biomarkers for Response to Neoadjuvant Chemoradiation in Rectal Cancer. *Int J Mol Sci*. 2017 Mar; 18(3): 573.
- Huang CM, Huang MY, Huang CW, et al. Machine learning for predicting pathological complete response in patients with locally advanced rectal cancer after neoadjuvant chemoradiotherapy. *Scientific Reports*. 2020 Jul; 10(1): 12555.
- Bibault JE, Giraud P, Housset M, et al. Deep Learning and Radiomics predict complete response after neo-adjuvant chemoradiation for locally advanced rectal cancer. *Sci Rep*. 2018 Aug; 8(1): 12611.
- Wei Q, Chen Z, Tang Y, et al. External validation and comparison of MR-based radiomics models for predicting pathological complete response in locally advanced rectal cancer: a two-centre, multi-vendor study. *Eur Radiol*. 2023 Mar; 33(3): 1906-17.
- Japanese Society for Cancer of the C, Rectum: Japanese Classification of Colorectal, Appendiceal, and Anal Carcinoma: the 3d English Edition [Secondary Publication]. *Journal of the anus, rectum and colon*. 2019 Oct; 3(4): 175-95.
- He K, Zhang X, Ren S, et al. Deep Residual Learning for Image Recognition 2016 IEEE Conference on Computer Vision and Pattern Recognition (CVPR), 2016: p770-8.
- Wakiya T, Ishido K, Kimura N, et al. CT-based deep learning enables early postoperative recurrence prediction for intrahepatic cholangiocarcinoma. *Scientific Reports*. 2022 May; 12(1): 8428.
- Fujita H, Wakiya T, Ishido K, et al. Differential diagnoses of gallbladder tumors using CT-based deep learning. *Ann Gastroenterol Surg*. 2022 Jun; 6(6): 823-32.
- Kanda T, Wakiya T, Ishido K, et al. Noninvasive Computed Tomography-Based Deep Learning Model Predicts In Vitro Chemosensitivity Assay Results in Pancreatic Cancer. *Pancreas*. 2024 Jan; 53(1): e55-61.
- Ojala M, Garriga GC. Permutation Tests for Studying Classifier Performance. *J Mach Learn Res*. 2010; 11: 1833-63.
- Stevenson ARL, Solomon MJ, Brown CSB, et al. Disease-free Survival and Local Recurrence After Laparoscopic-assisted Resection or Open Resection for Rectal Cancer: The Australasian Laparoscopic Cancer of the Rectum Randomized Clinical Trial. *Ann*

- Surg. 2019 Apr; 269(4): 596-602.
32. Fleshman J, Branda ME, Sargent DJ, et al. Disease-free Survival and Local Recurrence for Laparoscopic Resection Compared With Open Resection of Stage II to III Rectal Cancer: Follow-up Results of the ACOSOG Z6051 Randomized Controlled Trial. *Ann Surg.* 2019 Apr; 269(4): 589-95.
33. Hong YS, Park YS, Lim HY, et al. S-1 plus oxaliplatin versus capecitabine plus oxaliplatin for first-line treatment of patients with metastatic colorectal cancer: a randomised, non-inferiority phase 3 trial. *Lancet Oncol.* 2012 Nov; 13(11): 1125-32.
34. Yamada Y, Takahari D, Matsumoto H, et al. Leucovorin, fluorouracil, and oxaliplatin plus bevacizumab versus S-1 and oxaliplatin plus bevacizumab in patients with metastatic colorectal cancer (SOFT): an open-label, non-inferiority, randomised phase 3 trial. *Lancet Oncol.* 2013 Dec; 14(13): 1278-86.
35. Dekker E, Tanis PJ, Vleugels JLA, et al. Colorectal cancer. *Lancet.* 2019 Oct 19; 394(10207): 1467-80.

Journal of the Anus, Rectum and Colon is an Open Access journal distributed under the Creative Commons Attribution-NonCommercial-NoDerivatives 4.0 International License. To view the details of this license, please visit (<https://creativecommons.org/licenses/by-nc-nd/4.0/>).